

Theory for light emission from a scanning tunneling microscope

Peter Johansson

Institute of Theoretical Physics, Chalmers University of Technology, S-41296 Göteborg, Sweden

R. Monreal and Peter Apell*

Departamento de Física de la Materia Condensada, Universidad Autónoma de Madrid, E-28049 Madrid, Spain

(Received 22 August 1990)

We have calculated the rate of light emission from a scanning tunneling microscope with an Ir tip probing a silver film. We find a considerable enhancement of the rate of spontaneous light emission compared with, for example, inverse-photoemission experiments. This enhancement is the result of an amplification of the electromagnetic field in the area below the microscope tip due to a localized interface plasmon. One can estimate that one out of 10^4 tunneling electrons will emit a photon. We also find that the experimentally observed maximum in the light emission as a function of bias voltage is directly related to the detailed behavior of tip-sample separation versus bias voltage.

The scanning tunneling microscope (STM) is a useful tool for the analysis of different surface structures. In the usual mode of operation the STM is used to investigate the topography of the surface in question with remarkable resolution.¹

In this paper we give a theoretical treatment of a new way of using the STM where the light emitted from the microscope is detected. Gimzewski *et al.*² with an Ir-tip STM probing a silver film deposited on a Si substrate detected a strongly enhanced emission of light at photon energies around 2.5 eV.

The study of light emission from STM's is quite a new research field but light emission from other types of tunnel junctions has been investigated for a long time.³⁻⁵ In these experiments the tunnel junctions have had rough surfaces.

The common theme in the explanations of these experiments is that the tunneling electrons excite a surface plasmon which decays by sending out light. Due to the conservation of parallel momentum, surface plasmons on perfectly smooth surfaces cannot radiate. If, however, the translational invariance along the surface is broken by roughness or irregularities it becomes possible for the surface plasmon to send out light.⁶⁻⁸

The silver film used in the experiment by Gimzewski *et al.* was granular with a grain size of about 200 Å. Persson and Baratoff⁹ have recently studied theoretically the effect of this granularity on the light emission.

In this work we investigate what role the microscope tip itself plays in breaking the translational invariance along the surface and so enhancing the rate of light emission from the tunneling electrons.

Our calculation shows that the presence of the tip creates a localized interface plasmon mode in the region close to the tip. The rate of light emission is considerably enhanced for photon energies around 2.5 eV due to this resonance. We find that in a typical experimental situation the photon creation efficiency is of the order of 10^{-4} photons per electron. This efficiency is, considering the simplicity of our model, in reasonable agreement with ex-

perimental estimates.¹⁰

The calculation of the intensity of the emitted light from the tunneling electrons splits into two separate problems. One is the determination of the electromagnetic field in the vicinity of the tip giving us a measure of the strength of the coupling between tunneling electrons and the electromagnetic field. The other is the calculation of the fluctuations in the tunnel current that act as a source for the radiation. The largest amount of energy an electron can lose when tunneling is eU , where U is the bias voltage of the STM.

We will now derive an expression for the intensity of the emitted light using the reciprocity theorem of electrodynamics. The quantity we want to deduce is the radiated electric field $E(\mathbf{r}, \omega) \hat{\theta}$ at large distance from the STM tip given a certain current density near the tip $j(\mathbf{r}', \omega) \hat{z}$. What we do instead is that we place a δ -function current density $j_0 \delta^{(3)}(\mathbf{x} - \mathbf{r}) \hat{\theta}$ far away from the tip and then calculate the resulting electric field $E_{\text{ind}}(\mathbf{r}, \mathbf{r}', \omega) \hat{z}$ below the tip. See Fig. 1. The radiated electric field can be expressed as¹¹

$$E(\mathbf{r}, \omega) = (j_0)^{-1} \int d^3 r' E_{\text{ind}}(\mathbf{r}, \mathbf{r}', \omega) j(\mathbf{r}', \omega). \quad (1)$$

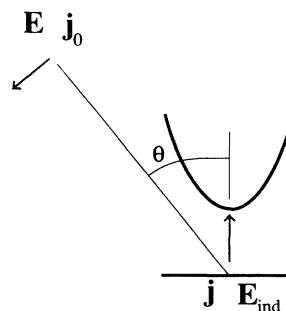


FIG. 1. The overall geometry (not to scale) of the field calculation. In the experiment the current j causes the field E far away from the tip. In our calculation j_0 is the source for E_{ind} . The different quantities are related according to the reciprocity theorem in Eq. (1).

E_{ind} in turn can be written as the product of two factors. The first factor is the magnitude of the plane wave that the δ -function source sends out into free space. The second factor $G(\mathbf{r}', \omega)$ holds in it all the dependence on the materials and geometry of the tip and the silver film including plasmon resonances. From electrodynamics we get¹¹

$$E_{\text{ind}}(\mathbf{r}, \mathbf{r}', \omega) = i \frac{\omega j_0}{c^2} \frac{e^{ikr}}{r} G(\mathbf{r}', \omega). \quad (2)$$

The current density $j(\mathbf{r}', \omega)$ in the z direction caused by the transition of an electron from an initial state $|i\rangle$ in the tip to a final state $|f\rangle$ in the sample is

$$j(\mathbf{r}', \omega) = -i(e\hbar/2m) \left(\frac{\partial \psi_f^*}{\partial z'} \psi_i - \psi_f^* \frac{\partial \psi_i}{\partial z'} \right) (\mathbf{r}'). \quad (3)$$

Here ψ_i and ψ_f are the wave functions of the two states involved. Their eigenenergies differ by the photon energy $\hbar\omega$.

Putting together what we have so far we get the following expression for the radiated electric field:

$$E(\mathbf{r}, \omega) = \frac{\omega}{c^2} \frac{e^{ikr}}{r} \frac{e\hbar}{2m} \int d^3r' G(\mathbf{r}', \omega) \left(\frac{\partial \psi_f^*}{\partial z'} \psi_i - \psi_f^* \frac{\partial \psi_i}{\partial z'} \right). \quad (4)$$

$$\int d^3r' G(\mathbf{r}', \omega) \left(\frac{\partial \psi_f^*}{\partial z'} \psi_i - \psi_f^* \frac{\partial \psi_i}{\partial z'} \right) = \delta_{\mathbf{k}_i, \mathbf{k}_f} (A/V) \int dz' G(z', \omega) \left(\frac{d\varphi_f^*}{dz'} \varphi_i - \varphi_f^* \frac{d\varphi_i}{dz'} \right) = \delta_{\mathbf{k}_i, \mathbf{k}_f} (A/V) M_{fi}. \quad (7)$$

Transforming the sums over initial and final states into momentum integrals, the differential power is found to be

$$\frac{d^2P}{d\Omega d(\hbar\omega)} = 2 \frac{c}{2\pi} \frac{e^2 \hbar^2 \omega^2}{4m^2 c^4} A \int \frac{dk_f}{2\pi} \int \frac{dk_i}{2\pi} \int \frac{d^2k_{\parallel}}{(2\pi)^2} |M_{fi}|^2 \delta(\epsilon_i - \epsilon_f - \hbar\omega). \quad (8)$$

The first factor of 2 comes from the spin summation. The momentum quantum numbers in the z direction k_i and k_f are both referring to the silver sample.

The quantity still needed to calculate the differential power is $G(\mathbf{r}', \omega)$. In this calculation we choose to describe the tip-sample geometry using the model shown in Fig. 2. The Ir tip has been replaced by an Ir sphere placed above a perfectly smooth Ag surface. The geometry is described by the radius R of the sphere and the tip-sample separation d . Solutions to the field calculation problem in the nonretarded limit in this geometry have been given in the literature.⁸ The virtue of this model geometry is that it describes in a correct way the curvature of the tip as seen from the silver surface. The fields of a localized interface plasmon are concentrated to the region between the STM tip and the silver surface and therefore it is most important to model the geometry in a correct way in that region. When it comes to describing the actual materials in the tip and in the sample we have used experimentally measured dielectric functions.¹³

Our calculation of $G(\mathbf{r}', \omega)$ is carried out in two steps. In the first step the presence of the sphere is ignored. We use the Fresnel formula to get the z component of the electric field that results from the reflection of the wave coming in from the source far away. In the second step of our calculation, the effect of the sphere on the electric field is determined in the nonretarded limit. We are al-

Adding the contributions from different transitions we find the total radiated power per unit solid angle and unit photon energy,

$$\frac{d^2P}{d\Omega d(\hbar\omega)} = \frac{c}{2\pi} \sum_{i,f} r^2 |E(\mathbf{r}, \omega)|^2. \quad (5)$$

In this expression $E(\mathbf{r}, \omega)$ is the radiated electric field caused by the transition from $|i\rangle$ to $|f\rangle$. To be able to calculate the integral in Eq. (4) we must know the wave functions entering the expression. In this work we describe the tunneling in an essentially one-dimensional picture.¹² We use wave functions that have a space dependence typical for free electrons in the tip and also in the sample. The fact that the tunneling occurs over a limited cross-section area around the tip apex is taken into account in the choice of quantization volume. This is taken to be a cylinder with cross-section area equal to the effective tunneling area A . Letting V denote the quantization volume the wave functions will have the space dependence

$$\psi = V^{-1/2} e^{ik_{\parallel} z} \varphi(z). \quad (6)$$

The function $\varphi(z)$ is calculated by solving the one-dimensional Schrödinger equation with a potential given by the shape of the barrier. Making use of Eq. (6) we get

lowed to perform a nonretarded calculation since the dimension of the sphere is much less than a visible-light wavelength. The second calculation is carried out using bispherical coordinates as described in the paper by Rendell and Scalapino.⁸ This leads to an equation system describing the coupling of the surface modes of an isolated sphere to each other due to the presence of the silver surface. The numerical solution of the equations system yields the result for the factor $G(\mathbf{r}', \omega)$.

We have calculated G for a number of experimentally reasonable sphere radii R , keeping the tip-sample separa-

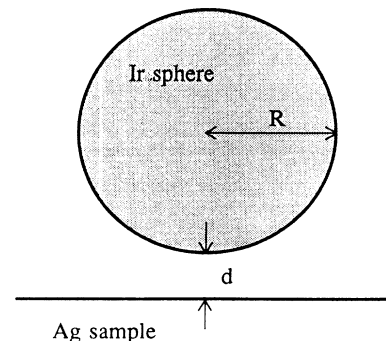


FIG. 2. The model geometry used in our calculation.

tion d constantly equal to 5 \AA which is a typical value in experiments. The results of our nonretarded model calculation does not depend on the actual size of the system, only on the proportions; thus R and d only enter the results in the combination d/R . A resonant maximum occurs in $G(\omega)$ showing that the field just below the tip can be enhanced by a factor of the order of 100. The resonance frequency depends on the tip radius, for $R=100 \text{ \AA}$ it is $\approx 3.1 \text{ eV}$ and for $R=300 \text{ \AA}$ it is $\approx 2.5 \text{ eV}$.

Materialwise, we have tried other sphere-sample combinations like a Ag sphere above a Ag sample and an Ir sphere above an Ir sample. These tests show quite clearly that all the structure in $G(\omega)$ originates primarily from the silver. The iridium tip plays a passive but yet very important role in breaking the translational invariance along the surface and thereby forming a localized interface plasmon mode.

Turning to the final calculation of the differential power we have found that the contributions to the matrix elements M_{fi} from the regions inside the silver and iridium are small compared to the contributions from the region between the tip and the sample. We have therefore approximated the matrix element by taking out $G(z',\omega)$ of the integral in Eq. (7) in our calculation of the differential power $d^2P/d\Omega d(\hbar\omega)$.

From the work by Pitarke, Flores, and Echenique¹² we know that the tip curvature plays an important role in determining the voltage-distance characteristics $d(U)$ of the STM when operating in the constant current mode. The main effect of the tip curvature is to increase the effective area seen by the tunneling electrons when either the applied bias or the tip radius is increased. To get the main features of the photon emission spectrum without resorting to lengthy numerical calculations we proceed in the simplest possible way as follows. First, we determine the voltage-distance characteristics for a constant tunneling current of 300 nA. The current is obtained as the product of the effective area and the current density. The effective area is taken from Ref. 12 and in the calculation of the current density we use wave functions calculated

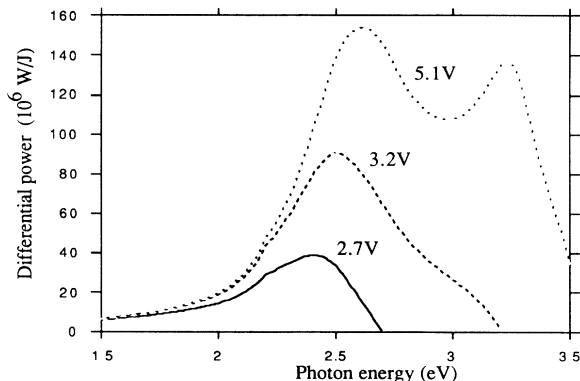


FIG. 3. The differential power $d^2P/d\Omega d(\hbar\omega)$ given in the direction $\theta=45^\circ$ for bias voltages 2.7 V ($d=4.8 \text{ \AA}$), 3.2 V ($d=4.92 \text{ \AA}$), and 5.1 V ($d=5.49 \text{ \AA}$). The tip-sample separation d is in each case chosen such as to give a tunnel current equal to 300 nA.

from a trapezoidal potential barrier. The values of the work functions and bandwidths are $\phi_1=4.7 \text{ eV}$ and $W_1=5.5 \text{ eV}$ for Ag and $\phi_2=5.8 \text{ eV}$ and $W_2=9.3 \text{ eV}$ for Ir. Using the voltage-distance characteristic so obtained and wave functions calculated from the above-mentioned potential we calculate the photon differential power.

In Fig. 3 we have plotted the final result for the differential power for three different biases. The angle of detection is 45° , and the sphere radius is 300 \AA for all the curves. The tip-sample separation and bias voltage are chosen in combinations such that the tunneling current is kept constantly equal to 300 nA.

We see when comparing these results with the experiment² that the curves have several features in common. The maximum intensity in the emitted light occurs at approximately the same photon energy. Moreover our results, similarly to the experimental results, show a trend of increasing ω_{max} with increasing bias voltage.

In Fig. 4 we have plotted the differential power at photon energy 2.4 eV as a function of bias voltage. Our results here agree qualitatively, however, not quantitatively with the experiment.² We get a maximum in the differential power for a bias voltage of 4–5 V. The experimental maximum occurred at about 3.5 V and for voltages above 4 V the intensity was considerably lower than the maximum intensity. Our explanation of the maximum is the following. As the bias voltage increases to values above 2.4 V the number of decay channels involving the emission of a 2.4 eV photon increases. This, of course, gives a differential power that grows with increasing bias voltage. However, when the bias voltage reaches values of 4–5 V the voltage-distance characteristics $d(U)$ changes from a linear increase for small U to an increase that is stronger than quadratic. This trend leads to a decrease in the light intensity because the function G roughly depends on d as $1/d$. Thus the curvature of the tip is essential not only when explaining the field enhancement in the tunneling region but it also gives an explanation to the maximum in the emitted light intensity as a function of bias voltage.

In summary, we have investigated theoretically the role the tip in a Ir-tip Ag-sample STM has on the spontaneous light emission from the microscope. We find that the

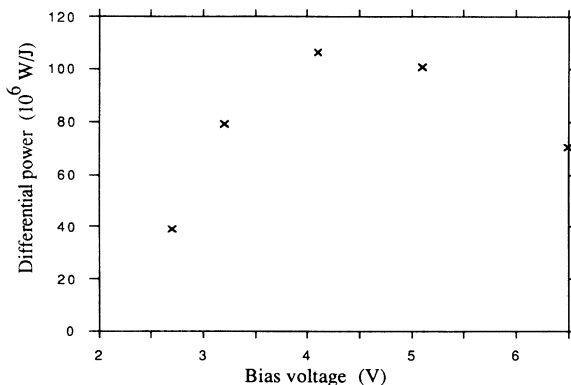


FIG. 4. The differential power $d^2P/d\Omega d(\hbar\omega)$ as a function of bias voltage U for photon energy $\hbar\omega=2.4 \text{ eV}$.

presence of the tip close to the sample surface creates a localized interface plasmon built up by surface charges of opposite polarity on the tip and the sample surface, respectively. This plasmon resonance leads to a considerable enhancement of the light emission from the tunneling electrons, with a quantum efficiency of the light emission of the order of 10^{-4} . The resonance frequency is sensitive to the tip curvature. Using a tip radius of 300 Å the calculated resonance coincides with the experimental resonance at a photon energy of 2.5 eV. We have also been

able to give a qualitative explanation for the experimentally observed maximum in the light emission as a function of bias voltage.

We have benefited from discussions with Göran Wendin, Bo Persson, Per Davidsson, and Fernando Flores. This project has been partially supported by the Swedish Natural Science Research Council and the Comisión Asesora de Investigación Científica y Técnica of Spain.

*Present and permanent address: Institute of Theoretical Physics, Chalmers University of Technology, S-41296 Göteborg, Sweden.

¹G. Binnig and H. Rohrer, *IBM J. Res. Develop.* **30**, 355 (1986).

²J. K. Gimzewski, J. K. Sass, R. R. Schlitter, and J. Schott, *Europhys. Lett.* **8**, 435 (1989).

³L. Lambe and S. M. McCarthy, *Phys. Rev. Lett.* **37**, 923 (1976).

⁴A. Adams and P. K. Hansma, *Phys. Rev. B* **23**, 3597 (1981).

⁵M. J. Bloemer, J. G. Mantovani, J. P. Goudonnet, D. R. James, R. J. Warmack, and T. L. Ferrell, *Phys. Rev. B* **35**, 5947 (1987).

⁶B. Laks and D. L. Mills, *Phys. Rev. B* **21**, 5175 (1980).

⁷K. Arya and R. Zeyher, *Phys. Rev. B* **28**, 4080 (1983).

⁸R. W. Rendell and D. J. Scalapino, *Phys. Rev. B* **24**, 3276 (1981).

⁹B. N. J. Persson and A. Baratoff, *Bull. Am. Phys. Soc.* **35**, 634 (1990).

¹⁰B. Reihl, J. H. Coombs, and J. K. Gimzewski, *Surf. Sci.* **211/212**, 156 (1989).

¹¹J. D. Jackson, *Classical Electrodynamics* (Wiley, New York, 1975).

¹²J. M. Pitarke, F. Flores, and P. M. Echenique, *Surf. Sci.* **234**, 1 (1990).

¹³P. B. Johnson and R. W. Christy, *Phys. Rev. B* **6**, 4370 (1972); J. H. Weaver, C. Krafka, D. W. Lynch, and E. E. Koch, *Physics Data No. 18-1* (Fachinformationszentrum, Karlsruhe, 1981).

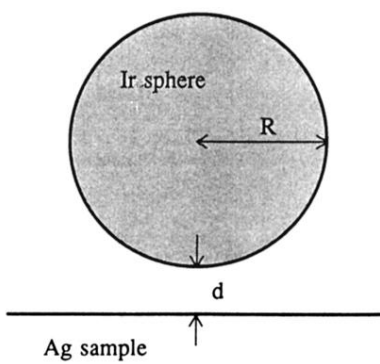


FIG. 2. The model geometry used in our calculation.